of dry air at 550 °C, conditions which would result in extensive dehydroxylation of the zeolite. According to the dehydroxylation model of Kühl[33] and others[34] cationic Al species are formed as the framework is dealuminated. In fact, NMR results have shown that extensive dealumination can occur at temperatures as low as 500 °C.[35] In the work presented here dehydroxylation and concomitant dealumination were avoided as was shown by the unit cell size of the catalyst after reaction. This is consistent with NMR results of Bösacek et al.[31] which showed that upon deammination at 400 °C under "shallow-bed" conditions only about 3 Al/uc were removed from the framework.

Although the acid strength of different types of zeolites may differ considerably because of changes in bond angle, bond length, etc., it is interesting to compare the specific activity for hexane cracking over a dealuminated Y sample and HZSM-5 having Si/Al = 26. The activities of 350 °C were 11.4 and 8.5 μmol/(g.min), respectively. Considering the differences in the zeolites the activities are quite similar. For cumene dealkylation the HZSM-5 catalyst was about twice as active as a comparable dealuminated Y, and for methanol dehydration the HZSM-5 was about 4 times as active.[18] Thus, the relative activity depends very much on the probe reaction.

(33) Kühl, G. H. In *Molecular Sieves*, Uytterhoeven, J. B., Ed.; Leuven University Press: Leuven, Belguim, 1973; p 227. *Molecular Sieves*, Vol. II, Katzer, J. R., Ed.; American Chemical Society: Washington, DC, 1979; ACS Symp. Ser. No. 40, p 96.
(34) Jacobs, P. A.; Beyer, H. K. *J. Phys. Chem.* **1979**, *83*, 1174.
(35) Klinowski, J.; Thomas, J. M.; Fyfe, C. A.; Gobbi, G. C. *Nature (London)* **1982**, 296, 533.

Conclusions

Hexane cracking is essentially a linear function of the lattice Al content over a range of Si/Al ratios from 4.6 to 255. To the extent that hexane cracking is a measure of strong acidity, the acid strength is constant over this range of Si/Al ratios. It is postulated that protons associated with isolated framework aluminum in the 4-rings give rise to the strong acidity which characterizes this material. The presence of aluminum in second-neighbor positions significantly decreases the acidity of a site. This is essentially the Dempsey–Mikovsky–Marshall (DMM) model of strong acidity.[6,7]

Consistent with this model, a normal H–Y zeolite, which has only a small amount of isolated tetrahedral aluminum, is relatively inactive for hexane cracking. Moreover, as described in part 1[15] the H–Y zeolite is relatively inactive for methanol dehydration, which requires only weak acid sites. This suggests that test reactions to characterize acid sites in zeolites need to be used with caution since a few strong acid sites may dominate the activity, even when a less-demanding reaction is employed.

Acknowledgment. This work was supported by the U.S. Army Research Office. The authors express their appreciation to Professor D. Kallő for helpful discussions related to this work.

Registry No. Hexane, 110-54-3.

Characterization of a New Iron-on-Zeolite Y Fischer–Tropsch Catalyst

Th. Bein,†

Institut für Physikalische Chemie der Universität Hamburg, Laufgraben 24, D-2000 Hamburg 13, FRG

G. Schmiester,

Institut für Atom- und Festkörperphysik der Freien Universität Berlin, Arnimallee 14, D-1000 Berlin 33, FRG

and P. A. Jacobs*

Laboratorium voor Oppervlaktechemie, Katholieke Universiteit Leuven, Kardinaal Mercierlaan 92, B-3030 Leuven (Heverlee), Belgium *(Received: October 3, 1985; In Final Form: December 26, 1985)*

Iron pentacarbonyl adsorbed on dry Na–Y zeolite can be oxidized at subambient temperatures into Fe_2O_3 located in the zeolite supercages (catalyst I). When catalyst I is hydrogen reduced at 575 K most of the iron has agglomerated externally to the zeolite (catalyst II). When the iron carbonyl is thermally decomposed in vacuo at 525 K, an iron phase with a very low degree of dispersion is again obtained (catalyst III). During a Fischer–Tropsch reaction most of the iron is transformed into a Hägg-type carbide phase, located externally to the zeolite. Catalysts II and III rapidly reach steady state and show a Schulz–Flory-type of product distribution, the Hägg carbide being the active phase. Catalyst I slowly moves to steady state and Schulz–Flory behavior. Product selectivity is only found on this catalyst during transient conditions. The physical information on the three catalysts before and after reaction was obtained with transmission electron microscopy and Mössbauer and EXAFS spectroscopies. These techniques supplied consistent and complementary evidence.

Introduction

Iron clusters can be introduced in zeolites via several indirect methods. Hydrogen reduction of Fe(II)-exchanged faujasite-type zeolites is only possible with aluminum-rich samples.[1,2] Therefore, Fe(II) reduction in Y-type zeolites was attempted with stronger reducing agents.[3,4] Alternatively, neutral iron complexes such as iron carbonyls can be adsorbed into the pores or cages of a large-pore zeolite and subsequently decomposed.[5-10] The thermolysis of iron carbonyl adsorbed on zeolites, depending on the exact decomposition method used, gives rise to discrete iron particle size distributions and dispersions.[11,12] These systems have been

† Present address: Central Research and Development, Experimental Station, E. I. Du Pont de Nemours & Co., Wilmington, Delaware 19898.

(1) Huang, Y. Y.; Anderson, J. R. *J. Catal.* **1975**, *40*, 143.
(2) Garten, R. L.; Delgass, W. N.; Boudart, M. *J. Catal.* **1970**, *18*, 19.
(3) Schmidt, F.; Gunsser, W.; Adolph J. *ACS Symp. Ser.* **1977**, *40*, 291.
(4) Lee, J. B. *J. Catal.* **1981**, *68*, 27.
(5) Ballivet-Tkatchenko, D.; Coudurier, G.; Mozzanega, H.; Tkatchenko, I. *Fundam. Res. Homogeneous, Catal.* **1979**, 257.
(6) Ballivet-Tkatchenko, D.; Coudurier, G. *Inorg. Chem.* **1979**, *18*, 558.
(7) Ballivet-Tkatchenko, D.; Chau, N. D.; Mozzanega, H.; Roux, M. C.; Tkatchenko, I. *ACS Symp. Ser.* **1981**, *152*, 187.
(8) Ballivet-Tkatchenko, D.; Coudurier, G.; Chau, N. D. *Stud. Surf. Sci. Catal.* **1982**, *19*, 123.

0022-3654/86/2090-4851$01.50/0

characterized till now by thermogravimetric,[13,14] in situ infrared,[13,14] and magnetic techniques.[11,12,15]

For catalyst preparation the carbonyl decomposition has definite advantages over hydrogen reduction of cation-exchanged Fe(II).[15] The activity of Y zeolite loaded with iron carbonyl has been investigated in a Fischer–Tropsch (FT) reaction.[5-8] The experiments were done in a batch reactor and, although in this way only "average" product distributions are obtained, it was concluded that the zeolite matrix was influencing the product distribution by decreasing suddenly the hydrocarbon growth rates at the carbon numbers 8–10. Similar results have been obtained with Ru clusters on NaY zeolites.[16-18] It remains therefore vital to decide on the exact influence of the zeolite on the FT selectivity.

In the present work, it was certified with several physical methods (Mössbauer and EXAFS spectroscopies, and transmission electron microscopy) that the FT active phase of the fresh catalyst was confined to the intracrystalline void space of zeolite Y. This catalyst was prepared by the iron carbonyl decomposition method. Reference zeolite-based iron catalysts containing substantial amounts of extra lattice iron particles were prepared as well. The physical characteristics of the steady-state catalysts were compared with fresh materials. This allowed us to draw pertinent conclusions on the way the Y zeolite matrix influences the FT selectivity.

Experimental Section

Materials. A synthetic Na–Y zeolite from Strem Chemicals was treated with an excess of a 0.1 M aqueous solution of NaCl, washed with distilled water till chloride-free, dried in air at 333 K, and stored in an atmosphere of 25% humidity. Iron pentacarbonyl ($Fe(CO)_5$) from Ventron with a purity of 99.5% was coldly distilled in the dark and stored over molecular sieve 5A. All gases used, CO, H_2, Ar, He, and O_2, were from L'Air Liquide and had a purity better than 99.99 vol%.

Methods. Catalyst Preparation. The moisture-saturated Na–Y zeolite was pelletized, crushed, and sieved. A grain size between 0.25 and 0.5 mm was used for further work. A 300-mg sample of this zeolite was loaded into a stainless steel tubular reactor with a 10-mm internal diameter. This reactor was first mounted in a large glass tube and connected to a grease-free gas handling and dosing system. The sample was degassed at 670 K, cooled to 293 K, and saturated with $Fe(CO)_5$ vapor. The iron pentacarbonyl equilibrium pressure at 273 K was 870 Pa. The Na–Y grains were equilibrated with the carbonyl for a period of 6 h. Thereafter, the Na–Y sample loaded with carbonyl was degassed to 1 mPa at 293 K over 1 h. This was done to remove excess carbonyl as well as the adsorbate from the outer surface of the zeolite crystals.[14] Subsequently, this sample was cooled to liquid nitrogen temperature and dry oxygen was admitted to the cold vessel at a pressure of 15 kPa. For a period of 10 h the vessel was allowed to warm to room temperature. The sample was again evacuated to 1 mPa as before and ultimately 100 kPa of dry oxygen was admitted. At this stage, the reactor was exposed to the open atmosphere and then was quickly mounted in the furnace of a catalytic high-pressure reactor unit. The catalyst thus prepared will be denoted as *Na–Y/FeO$_x$*. It contains 9% by weight iron, as determined afterward by X-ray fluorescence techniques. When this sample is reduced in a hydrogen flow of 0.9 L/h at 575 K, it is denoted as *Na–Y/FeO$_x$-RED*.

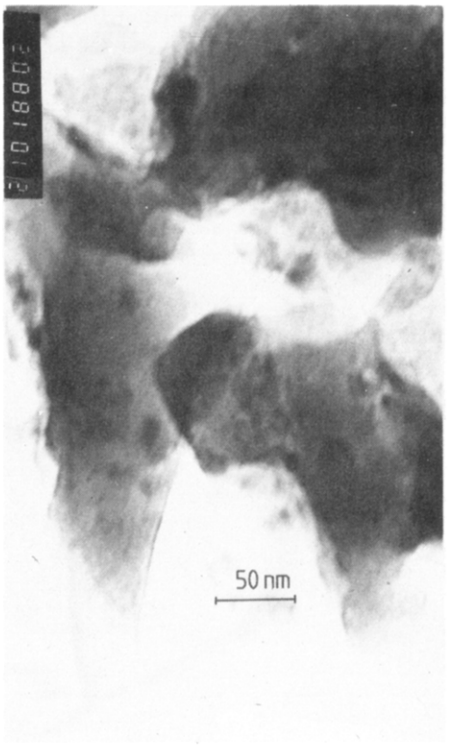

Figure 1. Transmission electron micrograph of sample Na–Y/FeO_x.

Dry Na–Y loaded with $Fe(CO)_5$ as described above was also heated under a vacuum of 1 mPa to 525 K. In this way, part of the adsorbed iron carbonyl is decomposed and another part is desorbed. The sample contains therefore only 6% iron and will be denoted further as *Na/Fe(0)*.

Catalytic Measurements. Catalytic experiments were performed in a high-pressure continuous-flow tubular reactor. The effluent vapors were transferred to the analytic section with a transfer line heated at 420 K. The analytical procedure has been described in detail.[19] It allowed accurate carbon mass balances (within ±2%), to be determined.[20] The reactor feed consisted of H_2, CO, and Ar in molar ratios of 55:40:5, respectively. The reaction pressure was 2.0 MPa and the total flow rate 1.8 L/h at the reactor entrance. The catalyst was activated in synthesis gas at 555 K. Product samples were taken periodically till catalyst steady state was reached.

Catalyst Characterization. Electron micrographs were taken with a Jeol JEM 200 CX instrument in the transmission mode (TEM). About 5 mg of sample was ground in an agate mortar and then suspended in 1 mL of ethanol (p.a.). The suspension was dripped on Fornvar grids and dried. An electron beam magnification between 50 000× and 300 000× was applied.

Mössbauer spectra of the 14.4-keV γ-resonance of iron were taken at temperatures between 1.8 and 300 K with a Fe(Rh) source. Samples for Mössbauer spectroscopy were prepared in a quartz reactor[21] under conditions that are similar to those applied in the catalytic reactor. Finally, they were embedded in paraffin so that sample transfer under inert conditions was possible. Thus, Mössbauer spectra were taken of samples representing the original chemical state of the catalysts before reaction.

EXAFS measurements of the K edge of iron were carried out at liquid nitrogen temperature with the spectrometer EXAFS II at HASYLAB (DESY, Hamburg, FRG).

Results and Discussion

Study of the Iron Phase on the Freshly Prepared Samples. Characterization of Highly Dispersed Na–Y/FeO$_x$. For more

(9) Nazar, L. F.; Ozin, G. A.; Hugues, F.; Godber, J.; Rancourt, D. *J. Mol. Catal.* **1983**, *21*, 313.
(10) Nagy, J. B.; van Eenoo, M.; Derouane, E. G. *J. Catal.* **1979**, *58*, 230.
(11) Schmidt, F.; Bein, Th.; Ohberich, U.; Jacobs, P. A. In *Sixth International Zeolite Conference*; Olson, D., Bisio, A., Eds.; Butterworth: London 1984; p. 151.
(12) Bein, Th.; Schmidt, F.; Jacobs, P. A. *Stud. Surf. Sci. Catal.* **1985**, *24*, 419.
(13) Bein, Th.; Jacobs, P. A.; Schmidt, F. *Stud. Surf. Sci. Catal.* **1982**, *19*, 111.
(14) Bein, Th.; Jacobs, P. A. *J. Chem. Soc., Faraday Trans. 1* **1983**, *79*, 1819.
(15) Bein, Th.; Schmidt, F.; Jacobs, P. A. *Zeolites* **1985**, *5*, 240.
(16) Nijs, H. H.; Jacobs, P. A.; Uytterhoeven, J. B. *J. Chem. Soc., Chem. Commun.* **1979**, 1095.
(17) Nijs, H. H.; Jacobs, P. A. *J. Catal.* **1980**, *65*, 328.
(18) Nijs, H. H.; Jacobs, P. A. *J. Catal.* **1980**, *66*, 401.
(19) Nijs, H. H.; Jacobs, P. A. *J. Chromatog. Sci.* **1981**, *19*, 40.
(20) Jacobs, P. A.; Willemen, K.; Leplat, L.; Uytterhoeven, J. B. *Energy Conservation in Industry*; VDI Verlag: Duesseldorf, Vol. 3, p 67.
(21) Bein, Th.; Schmiester, G.; Gunsser, W.; Schmidt, F. *Surf. Sci*, in press.

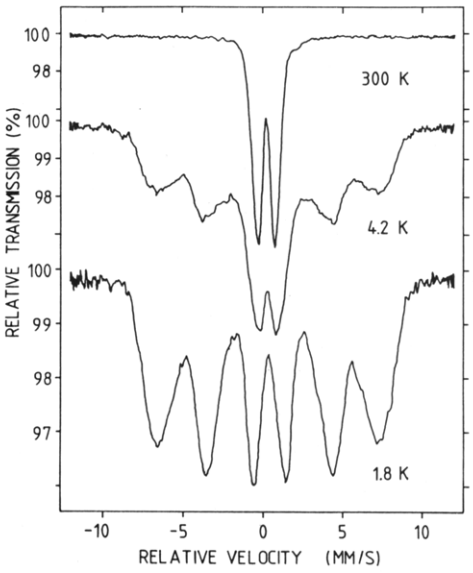

Figure 2. Mössbauer spectra of sample Na–Y/FeO_x measured at 300, 4.2, and 1.8 K. The lines are drawn by connecting all data points measured.

than 50 years it has been known that when oxygen reacts at room temperature with $Fe(CO)_5$ adsorbed on high surface area supports Fe_2O_3 is formed.[22] To avoid overheating during this reaction and consequently agglomeration of the supported species, the dry Na–Y zeolite containing on the average three molecules of the $Fe(CO)_5$ complex per faujasite supercage[13,14] was contacted with oxygen only at 77 K. Gradual oxidation then took place when the sample was allowed to warm to room temperature. Indeed, the cream color of the iron pentacarbonyl–zeolite adduct turned gradually to a light brown. This was the product that has been characterized by TEM, Mössbauer, and EXAFS techniques. An electron micrograph of such a sample, denoted as Na–Y/FeO_x, is shown in Figure 1. Even at the high magnifications applied, no resolved iron metal particles are visible on the zeolite support. This suggests that the FeO_x particles on Na–Y have an average size smaller than 2 nm. In agreement with the TEM data, an X-ray diffractogram (XRD) of this sample also shows no diffraction line attributable to FeO_x.

From the Mössbauer spectra of sample NaY/FeO_x shown in Figure 2, the following information can be derived:

i. At low temperatures, a symmetrical six-line pattern exists with a magnetic hyperfine line splitting of 42.8 T and an isomer shift (IS) of 0.3 mm s^{-1}.

ii. At higher temperatures, this pattern disappears, leaving only a symmetrical doublet with an IS of 0.3 mm s^{-1} and a quadrupole splitting of V_{zz} = 1.0 mm s^{-1}. V_{zz} was derived by raising the temperature from 1.8 to 300 K. In Table I are collected relevant Mössbauer data on iron-containing systems. It follows that in the Na–Y/FeO_x sample the presence of the following species can be excluded: iron(0) clusters or particles, iron carbides, Fe(II), and Fe(III) cations at exchangeable positions in the Y zeolite, and unreacted iron pentacarbonyl. This table indicates that the Mössbauer parameters of Fe_2O_3 either supported on NaY or on alumina are similar to those of the Na–Y/FeO_x zeolite. The values of the hyperfine field and the relaxation behavior of the system, however, suggest that very small particles of either α-Fe_2O_3 or γ-Fe_2O_3 are present. Since the value of the hyperfine field of α-Fe_2O_3 decreases with its particle size[23,25] in the size range below 10 nm, a more precise assignment based on Mössbauer data is not possible. Additionally, as a result of the broad spectral width, accurate numerical evaluation of the Mössbauer parameters is difficult. Further evidence for a simple oxide phase dispersed in the zeolitic cages will be presented when the evaluation of the EXAFS Fourier transforms is discussed.

TABLE I: Overview of Mössbauer Data of Different Iron Systems at Room Temperature

iron phase	hyperfine splitting/T	isomer shift[a]/mm s^{-1}	quad. splitting/mm s^{-1}	ref
Na–Y/FeO_x	42.8	0.3	1.0	
bulk iron	33.0	0.0		
Fe(0)/Na–Y	33.1	0.0		23
γ-Fe_2O_3/Na–Y	48.9	0.29 (Fe)		4
α-Fe_2O_3/Na–Y	49.6	0.34 (Co/Cu)		24
Fe_2O_3/Al_2O_3 (d < 10 nm)	(54.5)	0.32 (Fe)	0.46–0.98	25
α-Fe_2O_3/Na–Y	47.5[b]	0.44 (Fe)		23
ϵ-Fe_2C	23.8	0.34 (SNP)		26
	17.3	0.37 (SNP)		
Fe–C	26.5 ± 0.2	−0.03 ± 0.05		27
(martensite)	34.2 ± 0.2	0.02 ● 0.05		
	33.4 ± 0.2	0.01 ± 0.05		
ϵ-Fe_2C I	17.0 ± 0.3	0.20 ± 0.05		28
ϵ-Fe_2C II	23.7 ± 0.3	0.35 ± 0.05		
ϵ-Fe_2C III	13.0 ± 0.6	0.30 ● 0.05		
χ-Fe_5C_2	18.4 ± 0.3	0.30 ● 0.04		28
(Hägg)	22.2 ± 0.3	0.35 ± 0.04		
	11.0 ± 0.6	0.30 ± 0.08		
Fe_3C	20.8 ± 0.7	0.29 ± 0.02		29
Fe(II)/Na–Y		0.94 (Co/Cu)	2.32	30
Fe(II)/Na–Y		1.40 (Co/Cr)	2.29 ± 0.03	31
Fe(II)/Na–X		1.22 (Fe)	2.44 ± 0.03	32
		0.93 (Fe)	0.53	
Fe(III)/Na–Y		±0.05	0.9–1.2	24
$Fe(CO)_5$, 77 K		0.01 (Co/Fe)	2.52	33

[a] Relative to bulk iron (Fe), sodium nitropruside (SNP), Co/Cu, or Co/Fe. [b] At 5 K.

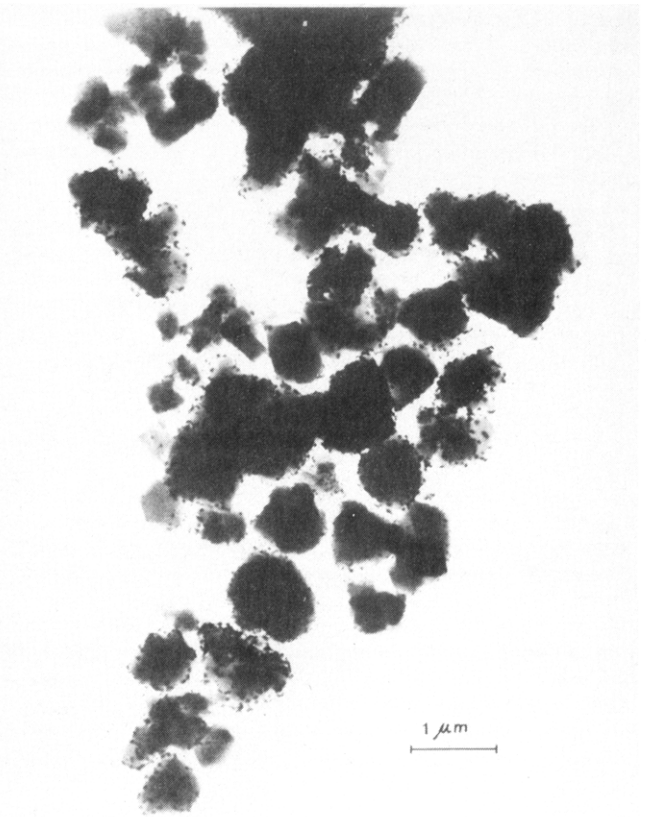

Figure 3. Transmission electron micrograph of sample Na–Y/Fe(0).

Characterization of Sample Na–Y/Fe(0). Thermal decomposition under vacuum of $Fe(CO)_5$ adsorbed on Na–Y zeolite

(22) *Gmelin's Handbuch der Anorganischen Chemie*; Springer Verlag: Berlin, 1930; Vol. Fe(B), p 444.

(23) Rancourt, D. G.; Daniels, J. M.; Nazar, L. F.; Ozin, G. A. *Proc. Conf. Magn. Hyperf. Interactions* **1983**.

(24) Wiedenmann, A.; Schmidt, F.; Gunsser, W. *Ber. Bunsen-Ges. Phys. Chem.* **1977**, *81*, 525.

(25) Kundig, W.; Bömmel, H.; Constabaris, G.; Lindquist, R. H. *Phys. Rev.* **1966**, *142*, 327.

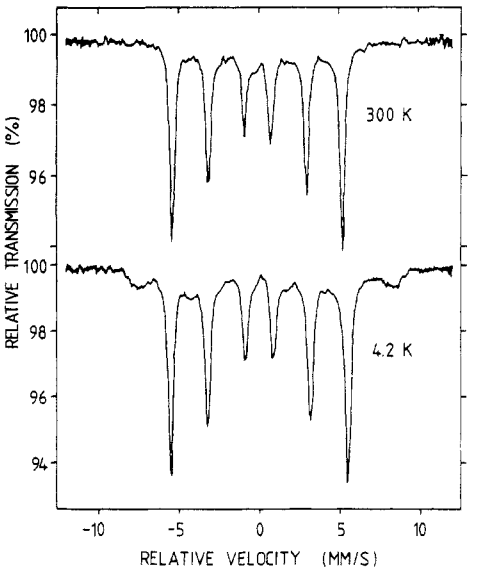

Figure 4. Mössbauer effect spectra of sample Na–Y/Fe(0) at 300 and 4.2 K.

shows an enhanced tendency to sinter compared to its rapid thermolysis under inert gas.[11] The electron micrograph of such a $Fe(CO)_5$–Na–Y zeolite adduct subjected to a slow temperature increase under vacuum is shown in Figure 3. It is seen that iron particles with an average size of about 30 nm are located at the outer surface of the zeolite crystals. The Mössbauer spectra on the same sample are given in Figure 4. A typical Fe(0) sextet with a magnetic hyperfine splitting of 33.0 T and a value of IS of 0.0 mm s^{-1} is obtained. These values are also observed for bulk iron (Table I). No relaxation behavior is encountered, since even at room temperature this sextet remains unchanged. This provides evidence for the existence of an almost pure Fe(0) phase with a particle size larger than the zeolite supercages. A small amount of iron(III) oxide, however, seems to be present on this sample since the weak lines have a hyperfine splitting comparable to sample Na–Y/FeO_x (compare Figures 2 and 4).

The Fourier transform of the EXAFS spectrum of Na–Y/Fe(0) is shown in Figure 5B and compared to that of Na–Y/FeO_x in Figure 5A. The EXAFS spectrum of sample Na–Y/Fe(0) resembles the pattern of bulk iron and had a nearest-neighbor distance (d_{nn}) of approximately 0.24 nm. For the Na–Y/FeO_x sample, the main EXAFS peak is found at a d_{nn} of approximately 0.18 nm. This distance is typical for iron(III) oxides.[22] The EXAFS data, therefore, are in line with conclusions from TEM and Mössbauer spectroscopy: on Na–Y/Fe(0) large iron particles located outside the zeolite crystals constitute the main iron-containing phase, while on Na–Y/FeO_x an Fe_2O_3 phase is finely dispersed in the zeolite cages.

Characterization of Sample Na–Y/FeO_x-RED. When sample Na–Y/FeO_x is hydrogen reduced at relatively high temperatures (575 K) for an extended period of time (50 ks), the sample turns black, large iron particles are observed in TEM, and the Mössbauer and EXAFS spectra typical for sample Na–Y/Fe(0) are found. There is no doubt that for this material the dominating iron phase consists of large iron particles located at the external surface of the zeolite crystals.

Characterization of Na–Y/FeO_x Used as a Fischer–Tropsch Catalyst. Sample Na–Y/FeO_x was used as a Fischer–Tropsch (FT) catalyst at 555 K till a steady-state conversion and stable product distribution was obtained. This used catalyst was then characterized with Mössbauer spectroscopy. These spectra recorded at 4.2 and 300 K, respectively, are shown in Figure 6. A striking difference is observed between these spectra and those of the fresh catalyst (Figure 2). Several new absorption lines in the inner range indicate that new iron species are generated during the CO hydrogenation reaction.

The outer lines of this spectrum at 4.2 K (Figure 6A) (at a distance of 8.13 mm s^{-1}) correspond to a magnetic hyperfine field

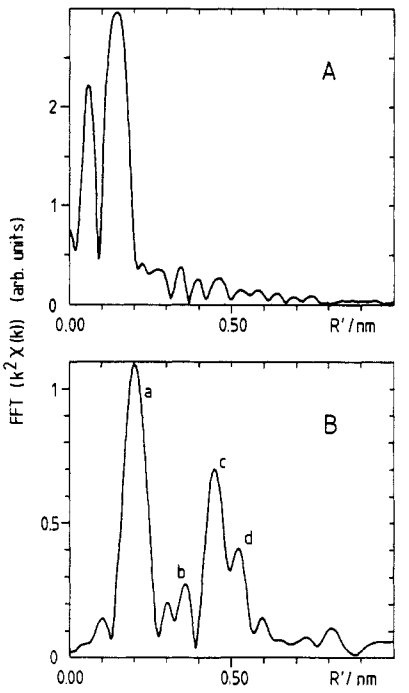

Figure 5. (A) Fourier transform of the EXAFS spectrum of sample Na–Y/FeO_x and (B) of sample Na–Y/Fe(0); (a) first and second, (b) third, (c) fourth and fifth, and (d) sixth nearest-neighbor shells (nns). The peak positions are shifted by 0.02–0.05 nm from the actual distances due to phase shift effects.

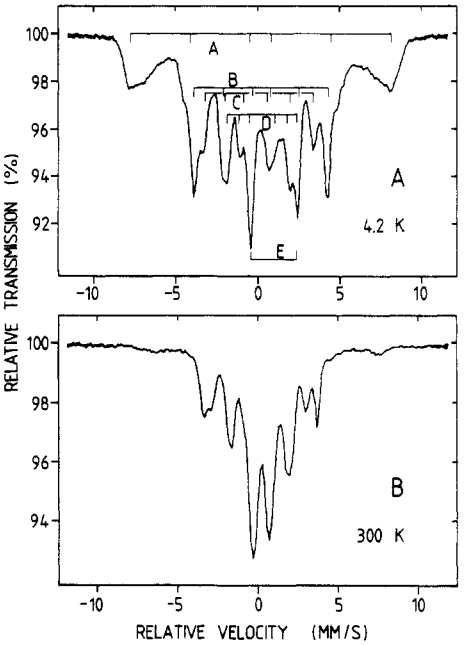

Figure 6. Mössbauer spectra measured at 4.2 K (A) and at 300 K (B) for sample Na–Y/FeO_x used in a FT synthesis for 72 ks at 555 K. Subsystems A–E are shown.

of 49.5 T, which is commonly found for iron(III) oxides (Table I). Since a relaxation is observed upon heating the sample to 300 K similar to that of sample Na–Y/FeO_x (Figure 2), these lines result from the presence of unreacted, highly dispersed Fe_2O_3. Since no relaxation model is presently available for this species, which would allow subtraction of the iron oxide fraction, spectral evaluation has to be done by graphic methods using a tentative assignment for other iron species. The result of this procedure is given in Table II. Three additional sextets can be found that fit the set of hyperfine fields obtained for Hägg carbide (Fe_5C_2) (subsystems B, C, and D of Table II and Figure 6A). There is no other iron carbide reported in the literature with hyperfine field values close to 21.9, 18.3, and 11 T (Table I). It is, however,

TABLE II: Characterization of Sample Na–Y/FeO_x after Syngas Conversion at 555 K by Mössbauer Spectroscopy[a]

sub-system	measuring temp/K	hyperfine splitting/T (±0.8)	isomer shift/mm s^{-1} (±0.1)	quad. splitting V_{zz}/mm s^{-1} (±0.1)	relax. behavior[b]
A	4.2[c]	49.5	0.2		+
B		25.2	0.2		–
C		20.7	0.1		–
D		13.0	0.2		–
E			1.0	2.8	–
A	300[c]		0.2	1.0	+
B		21.9	0.2		–
C		18.3	0.1		–
D		11.0	0.2		–
E			0.8	2.2	–

[a] Evaluated by graphic methods from the corresponding Mössbauer spectra of the catalyst after 72-ks time on stream. The unknown relaxation behavior of subsystem A prevented satisfactory reconstruction of the system by computer fits. [b] The outer absorption lines of subsystem A disappear upon warming the sample, whereas a strong inner doublet appears at 300 K. [c] See Figure 6.

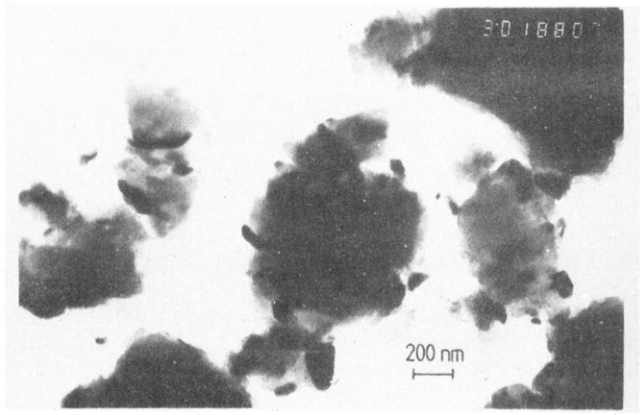

Figure 7. Transmission electron micrograph of sample Na–Y/FeO_x used in a FT synthesis for 72 ks.

well-known that magnetic hyperfine fields of iron carbides are subject to change with the nonstoichiometric change in population of iron nearest-neighbor sites by carbon atoms.[26,34] As a result of this effect and because the actual coordination sphere of the iron atoms in the small particles discussed here may have changed, the existence of other carbide phases (e.g., ϵ-Fe_2C) cannot be completely excluded.

A third iron phase is considered to be partially responsible for the two strongest lines at −0.4 and +2.4 mm s^{-1} in the spectrum (Figure 6A). Provided these lines represent a doublet, they are characterized by an isomer shift of 1.0 mm s^{-1} and a quadrupole splitting, V_{zz}, of 2.8 mm s^{-1}. The only reasonable assignment of these species seems to be to Fe(II) cations (Table I). In Fe(II) ion-exchanged Y zeolites, high-spin sixfold-coordinated Fe(II) ions located in the hexagonal prisms show IS values between 1.0 and 1.4 mm s^{-1} and V_{zz} between 2.29 and 2.44 mm s^{-1}. Fourfold-coordinated Fe(II) has its IS between 0.9 and 1.1 mm s^{-1} and V_{zz} between 0.53 and 0.58 mm s^{-1} (Table I). The subsystem E in the FT catalyst derived from NaY/FeO_x represents therefore sixfold-coordinated Fe(II) ions, possibly located in the hexagonal prisms of the zeolite.

TABLE III: Iron Zeolites as Fischer–Tropsch Catalysts at a Temperature of 555 K

catalyst	time on stream/h	% Co conversion	prod. distribn α	C no. range for distribn.
Na–Y/FeO_x	0.5	36.8	0.644	C_3–C_8
	15.0	27.9	0.781	C_3–C_{10}
	120.0	25.8	0.657	C_3–C_8
			0.875	C_3–C_{16}
Na–Y/Fe(0)	54.0	20.0	0.799	C_2–C_{17}
Na–Y/FeO_x-RED	60.0	35.0	0.781	C_3–C_{16}

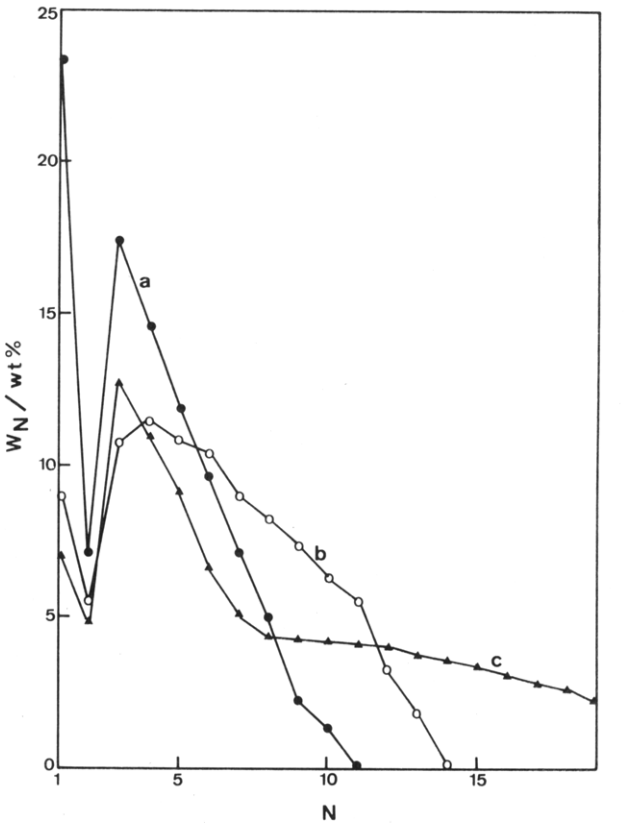

Figure 8. Hydrocarbon distribution over the different carbon numbers (N) during a FT experiment with sample Na–Y/FeO_x, after a time on stream of (a) 0.5 h, (b) 15 h, and (c) 120 h, respectively, and at 555 K.

The TEM of the used FT catalyst is shown in Figure 7. In contrast to the fresh catalyst on which no extrazeolitic phase could be observed (Figure 1), a great number of extrazeolitic particles are present now with an average diameter of about 50 nm. Since the Mössbauer spectrum of the small Fe_2O_3 particles remains virtually unchanged during reaction, these external large particles have to be associated with the formation of the iron carbide phase. This is further confirmed by the fact that the carbide sextets in the Mössbauer spectra (subsystems B, C, and D in Figure 6) do not relax when the sample temperature is increased to 300 K but show on the contrary a decreased value for the hyperfine field (Figure 6B). This indicates that larger particles are present.

It follows, therefore, that during a FT reaction a considerable fraction of the small Fe_2O_3 clusters encaged in a Y-type zeolite are transformed into Fe_xC with $2.0 < x < 2.5$. These carbide particles have an average diameter of about 50 nm and are located externally to the zeolite crystals. Another fraction of the Fe_2O_3 phase is reduced to sixfold-coordinated Fe(II) ions. A third fraction of the Fe_2O_3 clusters remains virtually unchanged during this reaction. The formation of iron carbides in general has been a well-discussed subject in relation to Fischer–Tropsch catalysis.[26,35–38] Even when the reaction is started with completely

(26) Pijolat, M.; Le Caer, G.; Perrichon, V.; Bussière, P. *Proc. Int. Conf. Appl. Mössbauer Effect* **1982**, 431.
(27) Moriya, T.; Ino, H.; Fujita, F. E. *J. Phys. Soc. Jpn.* **1968**, *24*, 60.
(28) Arents, R. A.; Maksimov, Yu. V.; Suzadalenev, I. P.; Imshennik, V. K.; Krupyanski, Yu. F. *Fiz. Met. Mettalloved.* **1973**, *36*, 277.
(29) Bernas, H.; Campbell, I. A. *J. Phys. Chem. Solids* **1967**, *28*, 17.
(30) Schmidt, F.; Gunsser, W.; Knappwost, A. *Z. Naturforsch. A. Phys., Phys. Chem., Kosmophys.* **1975**, *30A*, 1627.
(31) Delgass, W. N.; Garten, R. L.; Boudart, M. *J. Phys. Chem.* **1969**, *73*, 2970.
(32) Morice, J. A.; Rees, L. V. C. *J. Chem. Soc., Faraday Trans.* **1968**, *64*, 1388.
(33) Vertes, A.; Korecz, L.; Burger, K. *Mössbauer Spectroscopy*; Elsevier: Amsterdam, 1979.
(34) Vaishnava, P. P.; Montano, P. A. *J. Phys. Chem. Solids* **1982**, *43*, 809.

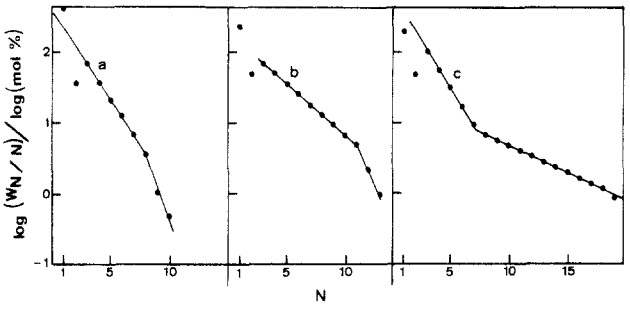

Figure 9. SF plot of the FT product distributions of Figure 8 after (a) 0.5 h, (b) 15 h, and (c) 120 h time on stream.

reduced iron, iron carbide phases similar to the presently encountered ones are formed under FT conditions.[26]

Behavior as Fischer-Tropsch Catalysts of the Fe/Na-Y Zeolites. Pertinent catalytic data for the three associations of iron with zeolite Na-Y are given in Figure 8 and in Table III. All catalysts were tested at medium conversion (Table III) so that considerable overheating of the reactor bed which occurs at high conversions is avoided but also that peculiar reaction selectivities which are sometimes associated with low conversions are not obtained.

Under such conditions it is seen (Table III) that the Na-Y/FeO_x catalyst slowly deactivates at increasing times on stream. More significant are the drastic changes in product selectivity associated with it. These changes are given in Figure 8 as distributions per carbon number fraction or in Figure 9 as a so-called Schulz-Flory (SF) plot. SF kinetics obey the following relation:[39]

$$W_N = N(1 - \alpha)^2\alpha^{N-1}$$

for which W_N corresponds to the product weight fraction with carbon number N. The chain-growth probability can be calculated from the slope of a log (W_N/N) against N plot. FT distributions sometimes deviate from SF behavior.[40] Since several artifacts may cause this deviation, of which non-steady-state behavior and deficiencies in the mass balance are often encountered, the material balance was checked carefully and found to be correct and the catalyst was followed till a stable product distribution was obtained. It is seen in Figure 8 that for longer times on stream, gradually heavier hydrocarbons appear in the product stream. It is also seen in Figure 9 that the growth factor of the hydrocarbon chains derived for the C_3–C_8 carbon number fraction increases steadily until ultimately a line with two distinct slopes is found. The latter behavior is typical for the presence of two discrete sets of sites. Relating this behavior to the physical nature of the catalyst investigated earlier, it can be assumed that the sites responsible for the first growth mechanism (α_1) are associated with the zeolite-supported Fe_2O_3 phase and those giving the α_2 growth rate with the extrazeolitic large Hägg-type carbide.

A deviation from SF behavior at higher carbon numbers has also been reported for other iron carbonyls physisorbed on Na-Y.[5-8] However, the present results show that under steady-state conditions a nonnegligible part of the iron has escaped from the zeolite matrix and consequently the typical zeolite-induced selectivity is partially lost. The other FT catalysts, Na-Y/Fe(0) and Na-Y/FeO_x-RED at steady state show perfect SF behavior (Figure 10) with very similar hydrocarbon growth rates (Table III). This is the expected behavior when the physical characterization of these catalysts is recalled: indeed, for both systems the major amount of the iron has escaped from the zeolite and agglomerated as large particles outside the crystals. It can be assumed that formation of a Hägg-type carbide phase mixed with Na-Y crystals occurs during the FT reaction.

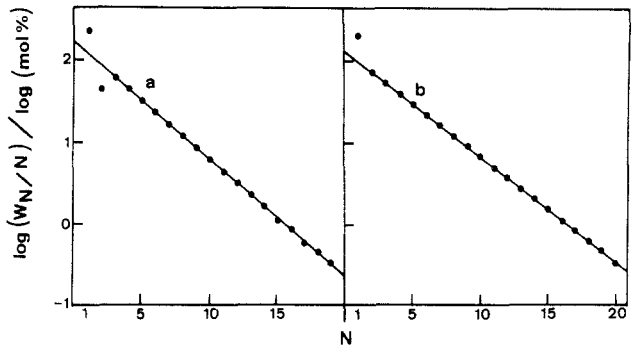

Figure 10. SF plot of the FT product distribution at steady state obtained at 555 K for (a) Na-Y/FeO_x-RED and (b), Na-Y/Fe(0) after a time on stream of 60 and 54 h, respectively.

Conclusions

In the present paper it is shown that when a Na-Y zeolite containing physisorbed iron pentacarbonyl is exposed to oxygen at 77 K and subsequently is heated to room temperature a highly dispersed Fe_2O_3 phase is formed in the zeolite supercages. When this sample is hydrogen reduced at 575 K, most of the iron is sintered into large particles located externally to the zeolite. When physisorbed pentacarbonyl is decomposed in vacuo at 525 K, a low dispersed iron phase located mainly outside the zeolite is formed.

The latter two materials behave as classical Fischer-Tropsch catalysts since the distribution of the hydrocarbons formed follows a Schulz-Flory behavior. The selectivity of the Fe_2O_3 phase in the Na-Y catalyst changes continuously until a steady state is reached. Such a steady state is characterized by a hydrocarbon distribution that is obtained by two different hydrocarbon growth rates. Physically, the steady-state catalyst only contains a remainder of the original Fe_2O_3 phase in the supercages, sixfold-coordinated Fe(II) ions and a new Hägg carbide phase located outside the zeolite crystals. It is therefore obvious to associate the high hydrocarbon growth rate in the FT reaction with the existence of this bulk carbide. Zeolite-induced FT selectivity seems therefore to exist only in transient conditions, unless migration and agglomeration of iron species during reaction is prevented.

Acknowledgment. T.B. acknowledges a grant from the Deutscher Akademischer Austauschdienst (DAAD) and support from the Belgian Ministry for Education, the Alfred Krupp von Bohlen and Halbach-Stiftung, and the DFG research project Schm. 597/1-2. P.A.J. acknowledges a permanent research position as Senior Research Associate from N.F.W.O.-F.N.R.S. (Belgium). Discussions with Prof. F. Schmidt (Hamburg) are very much appreciated. Financial support from the Belgian Government (Concerted Actions on Catalysis, Dientsten Wetenschapsbeleid) and from SFB 161 of DFG is also acknowledged.

Registry No. Fe, 7439-89-6.

(35) Amelse, J. A.; Butt, J. B.; Schwartz, L. H. *J. Phys. Chem.* **1978**, *82*, 558.
(36) Raupp, G. B.; Delgass, W. N. *J. Catal.* **1979**, *58*, 348.
(37) Niemantsverdriedt, J. W.; Van der Kraan, A. M.; Van Dijk, W. L.; Van der Baan, H. S. *J. Phys. Chem.* **1980**, *84*, 3363.
(38) Unmuth, E. E.; Schwartz, L. H.; Butt, J. B. *J. Catal.* **1980**, *63*, 404.
(39) Henrici-Olivé, G.; Olivé, S. *Angew. Chem.* **1976**, *88*, 144.
(40) Jacobs, P. A.; Van Wouwe, D. *J. Mol. Catal.* **1982**, *17*, 145.